$\frac{3}{2}\omega_0$ Radiation from the Laser-Driven Two-Plasmon Decay Instability in an Inhomogeneous Plasma

D. A. Russell and D. F. DuBois*

Lodestar Research Corporation, 2400 Central Avenue P-5, Boulder, Colorado 80301

(Received 28 February 2000; revised manuscript received 12 May 2000)

We present the results of the first reduced model simulations of the nonlinear development of the two-plasmon decay instability in an inhomogeneous plasma, including properties of the $\frac{3}{2}$ harmonic emission. A sharp increase in radiation and Langmuir turbulence fluctuation levels occurs above a threshold laser intensity that depends on initial fluctuation levels. We study the competition between the linear propagation of Langmuir waves in the density gradient and the nonlinear saturation due to the Langmuir decay instability. The secondary decay Langmuir waves can provide the dominant source of the radiation and are essential to explain experiments.

DOI: 10.1103/PhysRevLett.86.428 PACS numbers: 52.38.Bv, 52.35.Ra, 52.38.–r

The two-plasmon decay (TPD) instability, in which a laser photon with frequency ω_0 and wave vector $\mathbf{k}_0$ decays parametrically into a pair of Langmuir waves (LWs) with wave vectors $\mathbf{k}$ and $\mathbf{k}_0 - \mathbf{k}$ [1], appears to be the laser-plasma instability least controllable by beam smoothing [2]. It may be the most robust instability in direct-drive inertial fusion configurations, as evidenced by recent experiments on the Omega laser [3]. The emission of radiation near $\frac{3}{2}\omega_0$ has long been used [4] as the primary indicator of the presence of the TPD instability. In this Letter we present results from the first *ab initio* calculation of the spectrum of this radiation, for an inhomogeneous plasma, directly from a nonlinear model of the saturation of the TPD instability. This study illuminates several fundamental aspects of the role of nonlinearity in the saturation of parametric instabilities in an inhomogeneous plasma [5].

The extended Zakharov model of TPD used here is similar to that used by DuBois *et al.* [6]:

$$\nabla \cdot [2i\omega_{p0}(\partial_t + \nu_e \circ) + 3v_e^2\nabla^2 - \omega_{p0}^2(\delta n + \delta N)/n_0]\mathbf{E} = (e/4m_e)\nabla \cdot [\nabla(\mathbf{E}_0 \cdot \mathbf{E}^*) - \mathbf{E}_0\nabla \cdot \mathbf{E}^*] + S_E\,, \quad (1)$$

where $\mathbf{E}(x, y)$ is the complex vector envelope of the longitudinal electric field, $\frac{1}{2}\mathbf{E}\exp(-i\omega_{p0}t)$ + c.c., and $\mathbf{E}_0$ is the laser electric field envelope, here taken to be $\mathbf{E}_0 = \mathbf{e}_y|\mathbf{E}_0|\exp[ik_0x - i(\omega_0 - 2\omega_{p0})t]$. The reference electron plasma frequency is $\omega_{p0} = (4\pi e^2 n_0/m_e)^{1/2}$, and $v_e = (T_e/m_e)^{1/2}$ is the electron thermal velocity. For the slow density variation, $\delta n + \delta N$ represents the departure from the reference density, $n_0 = 0.23n_c$, where n_c is the laser critical density. The static background density profile is $N(x) \equiv [n_0 + \delta N(x)] = [0.23 + 0.04(2x/L_x - 1)]n_c$ and varies from $0.19n_c$ to $0.27n_c$ as x varies from 0 to L_x; the gradient scale length is $L_n = (23/8)L_x$. This is the "textbook" model of TPD in an inhomogeneous plasma which has been employed in all previous linear analyses. This Letter, we believe, presents the first nonlinear study of this fundamental problem and the first *ab initio* calculation of the $\frac{3}{2}\omega_0$ spectrum.

The low frequency density fluctuations, δn, provide the saturating nonlinearity in our model and evolve as ion acoustic waves (IAWs) driven by the ponderomotive pressure of the LWs,

$$[\partial_t^2 + 2\nu_i \circ \partial_t - c_s^2\nabla^2]\delta n = \nabla^2|\mathbf{E}|^2/16\pi m_i + S_{\delta n}\,. \quad (2)$$

The damping operators, $\nu_i \circ$ and $\nu_e \circ$, are local in $\mathbf{k}$ space and have the form $\nu_e = \nu_{\text{collisional}} + \nu_{\text{Landau-LW}}$ and $\nu_i = \nu_{\text{Landau-IAW}}$, where all terms are functions of $|\mathbf{k}|$ [6] for the fixed Maxwellian electron and ion velocity distribution functions assumed here. $c_s = \sqrt{(ZT_e + 3T_i)/m_i}$ is the IAW speed.

The well-known TPD convective growth rate [6] follows from the linearization of Eq. (1) with the term $\delta n + \delta N$ omitted and is maximized at the intersections of the hyperbolae $k_y^2 = k_x(k_x - k_0)$ with the circle given by frequency matching at a given density, $\Omega(x) \equiv \omega_0 - 2\omega_p(x) = \omega_{p0}\frac{3}{2}\lambda_{De}^2[k^2 + |\mathbf{k}_0 - \mathbf{k}|^2]$. These four most unstable wave vectors are $[k_x(x), k_y(x)] = [\frac{1}{2}k_0 \pm k_{De}\sqrt{\Omega(x)/6\omega_{p0}}\,, \pm\sqrt{k_{De}^2\Omega(x)/6\omega_{p0} - k_0^2}\,]$, where $k_{De} = 1/\lambda_{De} = \omega_{p0}/v_e$. They represent two pairs of TPD daughter waves, each pair composed of a LW propagating up the gradient and one propagating down, shifted in frequency from $\omega_0/2$ by

$$\Delta\omega_{3/2} \equiv \omega_{\text{LW}} - \omega_0/2 = \pm\sqrt{3/8}\,k_0v_e\sqrt{\Omega(x)/\omega_{p0}}\,. \quad (3)$$

The blueshifted (+) LW is forward-propagating, and the redshifted (−) LW is backward-propagating. This shift is conserved by WKB propagation.

We performed a series of two-dimensional (2D) simulations for the following parameters of a carbon plasma: laser wavelength $\lambda_0 = 1.06\ \mu$m, electron temperature $T_e = 0.8$ keV, ion charge state $Z = 6$, $m_i/m_e = 12 \times 1836$, and $L_n = 200\ \mu$m [7]. We used an IAW damping-to-frequency ratio of $\nu_{i0} \equiv \nu_i(k)/kc_s = 0.1$. The simulation cell had $L_x = 70\ \mu$m and $L_y = 22\ \mu$m. The

 0031-9007/01/86(3)/428(4)$15.00

time–random-phase Cerenkov noise sources, S_E and $S_{\delta n}$, maintain homogeneous, equilibrium levels of $\langle|\mathbf{E}(x,y)|^2\rangle/8\pi n_0 T_e = \langle\delta n(x,y)^2\rangle/n_0^2 = 2.8 \times 10^{-5}$, with the laser turned off. (These noise levels are appropriate for an infinite-volume plasma with 600 electrons per Debye cube.) The laser pump intensity was held fixed at various indicated values. Pseudospectral methods were used with periodic boundary conditions. In the x direction, LWs are reflected at higher densities, and they are absorbed by strong Landau damping at lower densities, so that there is naturally very little cross talk between periodic cells [5].

Figure 1 displays power spectra of LW fluctuations as a function of x and $\Delta\omega_{3/2}$ from a simulation of Eqs. (1) and (2) for a laser intensity $I_0 = 3.4 \times 10^{13}$ W/cm^2, below the numerically determined linear absolute instability threshold, and starting from thermal equilibrium levels (above) for $\langle|\mathbf{E}|^2\rangle$ and $\langle\delta n^2\rangle$. In this regime, IAWs play a negligible role in mediating LW behavior; this is TPD in the linear, convective regime. The solid maximal-gain curves shown in the figure are computed from Eq. (3) using the linear density profile. The bright areas correspond to the most intense LWs and roughly parallel the solid curves. The upper, forward-propagating, intense LWs start just to the left of the maximal-gain curves and propagate, at constant frequency, $\Delta\omega_{3/2} > 0$, farther to the right of these curves until they are damped or reflected. The waves are amplified on crossing the maximal-gain curves, as expected for locally matched, convectively amplified, LWs in a density gradient. For the lower curves, with $\Delta\omega_{3/2} < 0$, the picture is the same with directions of propagation reversed. The locus of reflection points for the forward-propagating LWs is shown as a solid white curve as well, partially occluded by the upper set of white disks that represent $\frac{3}{2}\omega_0$ emission by these forward-propagating, blueshifted LWs (see below). Only those LWs born nearest to reflection actually reach it with significant intensity despite strong collisional absorption. The redshifted LWs, $\Delta\omega_{3/2} < 0$, propagate without reflection down the density gradient until absorbed by Landau and/or collisional dissipation.

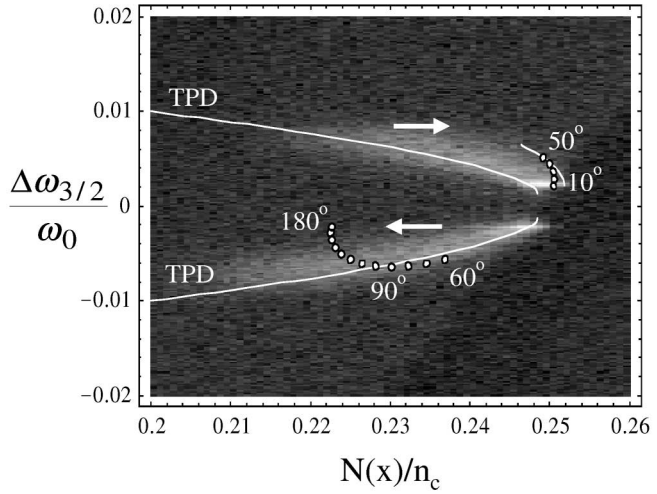

FIG. 1. Power spectra of LW fluctuations, $\langle|\mathbf{E}(x,\omega)|^2\rangle$, for the convectively saturated TPD instability. The laser intensity is $I_0 = 3.4 \times 10^{13}$ W/cm^2, and the laser propagates from left to right. The position is labeled by background density, $N(x)/n_c$, and the frequency origin is taken to be $\omega_0/2$, as discussed in the text, along with other parameters of the simulation. Maximal-gain curves are denoted "TPD."

The local current density driving the emitted radiation near $\frac{3}{2}\omega_0$ is the transverse component of $\mathbf{J}^{3/2} = -e \times [\mathbf{E}_0\nabla\cdot\mathbf{E}]\exp[-i(\omega_0 + \omega_{p0})t]/(16\pi i\omega_0 m_e)$ + c.c. [6]. Its $(\omega,\mathbf{k})$ spectrum thus provides information about LW fluctuations. It is well known that wave number and frequency matching constrain the LW $\mathbf{k}$ vectors that can couple to the $\frac{3}{2}\omega_0$ emission to lie on the "radiation circle" [8], $|\mathbf{k}_0 + \mathbf{k}| = k_{3/2} \cong \sqrt{8/3}\,k_0$. The frequency of the emitted light is $\omega_{3/2} = \omega_0 + \omega_{\rm LW}(\mathbf{k})$ and is shifted from the reference frequency $\frac{3}{2}\omega_0$ by $\Delta\omega_{3/2} \equiv \omega_{3/2} - \frac{3}{2}\omega_0 = \omega_{\rm LW}(\mathbf{k}) - \frac{1}{2}\omega_0$, as in Eq. (3).

For LWs born on the maximal-gain curves, k_y is given above as a function of x, as is the shift $\Delta\omega_{3/2}$. Both are conserved by WKB propagation; in particular, $k_y = (\mathbf{k}_{3/2})_y = k_{3/2}\sin(\theta)$, where θ is the angle of emission with respect to $\mathbf{k}_0$. Thus, given the angle of emission, we can find the LW birth density and then the density at emission from WKB propagation, in addition to the shift expected at that emission angle. The white disks in Fig. 1 locate $\frac{3}{2}$-harmonic radiation with respect to shift and emission density for various emission angles.

At $\theta = \cos^{-1}(\sqrt{3/8}) = 52.2°$, $k_x = 0$ on the radiation circle, so to emit radiation at larger (smaller) angles, LWs must be propagating down (up) the gradient. The upper set of white disks in Fig. 1 (i.e., those for which $\Delta\omega_{3/2} > 0$) locates potential emission by WKB LW packets, born on the upper maximal-gain TPD curve, that can propagate without reflection to the radiation circle, as indicated by the right-pointing arrow in the figure. Blueshifted emission at angles greater than 52.2° is negligible in the present case because the required backpropagating LWs are strongly absorbed by collisional damping. Blueshifted, backscattered light *from linear TPD alone* is expected to be very weak, contrary to many experimental observations.

The maximal-gain curve and emission disks for the redshifted light are shown in the lower half of Fig. 1. Red-shifted emission from TPD LWs dominates blueshifted emission for $\theta > 90°$. Although red LWs appear to couple locally at $\theta \sim 90°$, there is no transverse component of the current density and no emission at 90°, in fact, for the strictly linear $\delta N(x)$ and plane-wave laser profile assumed here.

Close to the quarter-critical density, red LWs appear to couple directly to the radiation. As the quarter-critical density is approached from below, the redshifted LW $\mathbf{k}$ vector vanishes, and the WKB analysis breaks down. In contradiction to the (invalid) WKB prediction, we typically find redshifted forward emission from linear TPD alone, observed over a wider range of forward angles with increasing laser intensity.

In Fig. 2 the power spectrum of LW fluctuations is shown from a simulation for the same parameters and initial conditions as in Fig. 1, but with a slightly higher laser intensity, $I_0 = 3.5 \times 10^{13}$ W/cm^2, just above the threshold for absolute TPD instability. Here two new solid curves are drawn indicating the loci of LWs resulting from the Langmuir wave decay instability (LDI) of the primary TPD LWs [5]. The curves are drawn using only the unmodified density profile, $N(x)$. Also drawn are points on the radiation circle that can be reached by propagation of these LDI waves. The backward-propagating LDI waves, resulting from the decay of forward-propagating TPD waves, now have significant intersections with the radiation circle, even without propagation, and engender strong, backward-emitted, blueshifted $\frac{3}{2}\omega_0$ light. The forward-propagating LDI waves can likewise couple locally to forward-emitted, redshifted light for $\theta < 52.2°$.

Notice that LW spectral energy is spread down in frequency, away from the TPD-LDI reference curves in Fig. 2, as the (unperturbed) quarter-critical density is approached from below. This spreading is due to turbulent profile modification driven by LW collapse. Collapse is most efficiently nucleated by the red TPD LWs near quarter-critical density [5] where, once the strong turbulence is excited, it is difficult to distinguish between LWs born of TPD, LDI, or collapse; TPD and LDI spectra tend to coalesce, and the LW dispersion tends to become distinctly nonlinear. Thus the origins of the redshifted, forward-emitted light, in particular, are manifold in the turbulent state. Nevertheless, where TPD and LDI LWs can be distinguished, *the nonlinearly produced LDI waves drive more blueshifted, backscattered light and more redshifted, forward-scattered light than the primary, linearly unstable TPD waves.*

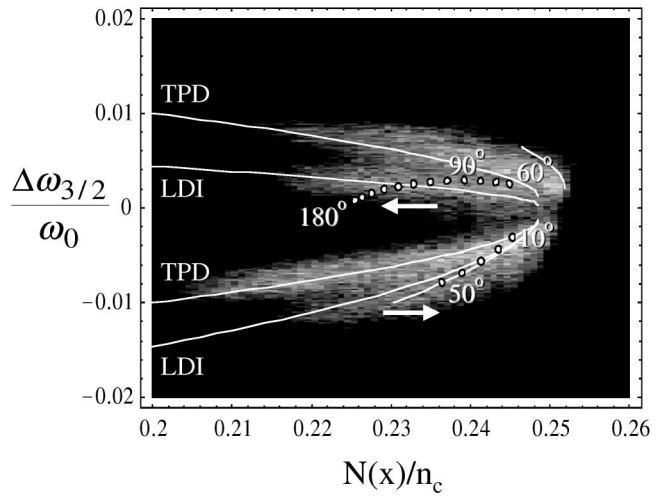

FIG. 2. $\langle|\mathbf{E}(x,\omega)|^2\rangle$, as in Fig. 1, but for the *nonlinearly* saturated TPD instability. The laser intensity is $I_0 = 3.5 \times 10^{13}$ W/cm^2. Decay of the primary LWs on the maximal-gain curves of Fig. 1 produces secondary LWs on the curves denoted "LDI" here.

In Fig. 3 (inset) we plot the intensity of the transverse component of the current density fluctuations on the radiation circle averaged over forward- and over backward-emission angles separately. All simulations for this figure were started from strong-turbulent, superthermal levels of fluctuations, and the turbulence was self-sustaining for laser intensities greater than 2.6×10^{13} W/cm^2. This "inflation" threshold lies well below the absolute instability threshold (approximately 3.5×10^{13} W/cm^2). For intensities between these two threshold values two states are possible (i.e., there is hysteresis), depending on initial conditions: either the strong-turbulent, or *inflated,* state or the weak regime of near-linear, convective TPD [5]. The intensity of $\frac{3}{2}\omega_0$ current density fluctuations increases dramatically as the LDI turns on for intensities above the inflation threshold (and also increases at fixed intensity with IAW damping ν_{i0} [5]).

Young and Moody [7] observed the emergence of a blueshifted component of the backemitted $\frac{3}{2}\omega_0$ radiation with increasing I_0. This appears to be consistent with our observation that the backscattered, blueshifted component emerges as the inflation threshold is exceeded. This is illustrated in Fig. 3. However, the angular dependence of the current density spectra in these simulations is not in good agreement with the radiation spectra detected remotely in the experiments. For example, Young and Moody observe a strong redshifted component at $\theta = 180°$, whereas we observe a dominant blue component. They also see a smoother angular dependence in the backward direction, including emission at $\theta = 90°$ for which the theory predicts zero emission. (Glenzer finds that whether or not

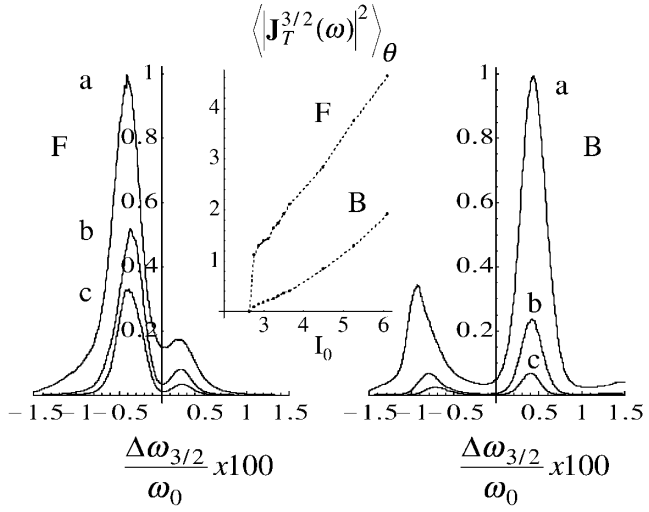

FIG. 3. Power spectra of $\frac{3}{2}\omega_0$ transverse current density fluctuations averaged over forward-scattered angles (F) and over backward-scattered angles (B), as indicated, for (*a*) $I_0 = 6.1$, (*b*) $I_0 = 3.5$, and (*c*) $I_0 = 2.75 \times 10^{13}$ W/cm^2. Spectra are normalized by the maximum value(s) in (*a*). In the inset we plot the intensity of the fluctuations averaged over frequency and over forward- and backward-emission angles, $\langle|\mathbf{J}_T^{3/2}|^2\rangle_{\omega,\theta}$, in units of $(en_0v_e)^2 \times 10^{-10}$, as a function of laser intensity in units of 10^{13} W/cm^2.

the strongest spectral feature is redshifted or blueshifted is unpredictable in time at a fixed angle of detection, in gas-bag experiments at NOVA [9].) Such discrepancies likely originate in the difficulty of inferring remotely detected radiation spectra from local current density fluctuation spectra when the experimental plasma density profile in the turbulence region is unknown.

A possible shortcoming of the modeling may be our failure to account for nonlocal heat transport at the longer wavelengths in this relatively low-temperature regime. According to simple "static" models [10], this effect appears to be marginal for IAWs that participate in backward emission through LDI. This is a topic for future research.

Now consider a CH plasma at a higher electron temperature, motivated by envisaged long scale-length plasma experiments at Omega [11]: $\lambda_0 = 0.351\ \mu$m, $T_e = 4.0$ keV, $L_n = 750\ \mu$m, and $\nu_{i0} = 0.1$, corresponding to $T_e/T_i = 2.5$. The simulation cell had $L_x = 260\ \mu$m and $L_y = L_x/4$, and we took $I_0 = 3.7 \times 10^{14}$ W/cm^2, about 4 times the threshold laser intensity for absolute instability. Figure 4(a) shows the $\frac{3}{2}\omega_0$ emission observed [11] from a spherical target uniformly irradiated by 60 laser beams for which there were many emission angles in the range $0 < \theta < 90°$ possible at the detector. Figure 4(b) shows the computed spectrum, averaged over forward angles; in this higher-T_e regime, the Landau damping of the backward-propagating LWs is so high that no backward emission is predicted. Both spectra show a more intense redshifted peak and have roughly the same ratio of redshifted-to-blueshifted intensities. But the separation of peaks is about twice as large in the simulation. The red-blue separation is proportional to $v_e \sim \sqrt{T_e}$ [see Eq. (3)] and also increases with the angle of emission *and with laser intensity,* e.g., see Fig. 3. It is likely that the experimental spectrum represents a sampling of the current density spectrum that is not uniform with forward-emission angle, unlike the sampling used for Fig. 4(b). The effective temperature in the turbulence region of the experiment was probably less than 4 keV [11], and the actual experimental intensity may have been less than assumed here. Finally, we note that the intensity of the $\frac{3}{2}\omega_0$ radiation has been observed to increase sharply with laser intensity in the experiments [11], possibly as the inflation threshold indicated in Fig. 3 is crossed.

In summary, we have presented the first 2D simulation results for the fundamental textbook problem of the nature of Langmuir turbulence induced by the saturation of the TPD instability of a plane-wave laser in a linear density profile. We find that the unstable LWs are convectively saturated along the maximal-gain curves in the density profile even when the system is above the absolute instability threshold. The signatures of the $\frac{3}{2}\omega_0$ emission spectra are strongly affected by the waves excited in the nonlinear saturation of the TPD instability. We have shown that there is a discontinuous change in the behavior of the emission at a nonlinear laser threshold that includes the excitation of the LDI [5]. Several improvements needed for more realistic modeling of experiments are evident. In particular, more complex models for the laser and density profile, possibly including the effects of nonlocal heat transport, should be employed in a stronger effort to make contact with the observed angular dependence of the emission.

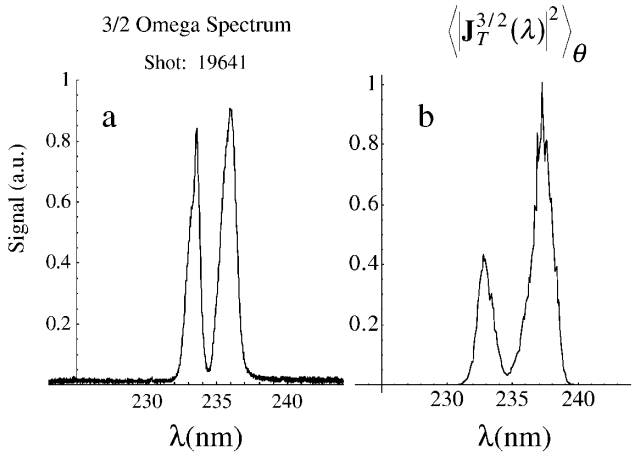

FIG. 4. Power spectra of (a) $\frac{3}{2}\omega_0$ radiation observed at the Omega Laser Facility and of (b) the $\frac{3}{2}\omega_0$ transverse current density fluctuations from our simulation for similar parameters (see text) averaged over forward-scattered angles, $|\theta| < 90°$. Both are plotted as functions of wavelength; (a) is in arbitrary units and (b) is normalized by its maximum value.

We thank P. Y. Young, J. D. Moody, S. Glenser, C. Stoeckl, R. E. Bahr, and W. Seka for allowing us to quote their data, some of which was unpublished at the time of this writing, and for helpful discussions. This research was supported by U.S. DOE High-Energy-Density Science Grant No. DE-FG03-98DP00205.

*Also at Los Alamos National Laboratory, MS B213, Los Alamos, New Mexico 87545.

[1] M. V. Goldman, Ann. Phys. (N.Y.) **38**, 117 (1966).
[2] T. A. Peyser *et al.,* Phys. Fluids B **3**, 1479 (1991).
[3] C. Stoeckl *et al.,* Bull. Am. Phys. Soc. **44**, 27 (1999); W. Seka *et al.,* Bull. Am. Phys. Soc. **44**, 25 (1999).
[4] W. Seka *et al.,* Phys. Fluids **28**, 2570 (1985).
[5] D. A. Russell and D. F. DuBois (to be published). Here more detailed results from these studies are presented concerning the properties of the TPD-excited Langmuir wave turbulence.
[6] D. F. DuBois, D. A. Russell, and H. A. Rose, Phys. Rev. Lett. **74**, 3983 (1995).
[7] P. Y. Young and J. D. Moody (private communication).
[8] J. Meyer and Y. Zhu, Phys. Rev. Lett. **71**, 2915 (1993); J. Meyer, Y. Zhu, and F. L. Curzon, Phys. Fluids B **1**, 650 (1989).
[9] S. Glenzer (private communication).
[10] D. S. Montgomery, R. P. Johnson, H. A. Rose, J. A. Cobble, and J. C. Fernández, Phys. Plasmas **84**, 678 (2000); H. A. Rose and D. F. DuBois, Phys. Fluids B **4**, 1394 (1992).
[11] C. Stoeckl, R. E. Bahr, and W. Seka (private communication).